Time history prediction of direct-drive implosions on the Omega facility

S. Laffite, J. L. Bourgade, T. Caillaud, J. A. Delettrez, J. A. Frenje, F. Girard, V. Yu. Glebov, T. Joshi, O. Landoas, G. Legay, S. Lemaire, R. C. Mancini, F. J. Marshall, L. Masse, P. E. Masson-Laborde, D. T. Michel, F. Philippe, C. Reverdin, W. Seka, and V. Tassin

Citation: Physics of Plasmas **23**, 012706 (2016); doi: 10.1063/1.4939833
View online: http://dx.doi.org/10.1063/1.4939833
View Table of Contents: http://scitation.aip.org/content/aip/journal/pop/23/1?ver=pdfcov
Published by the AIP Publishing

Time history prediction of direct-drive implosions on the Omega facility

S. Laffite,[1] J. L. Bourgade,[1] T. Caillaud,[1] J. A. Delettrez,[2] J. A. Frenje,[3] F. Girard,[1] V. Yu. Glebov,[2] T. Joshi,[4] O. Landoas,[1] G. Legay,[5] S. Lemaire,[1] R. C. Mancini,[4] F. J. Marshall,[2] L. Masse,[1] P. E. Masson-Laborde,[1] D. T. Michel,[2] F. Philippe,[1] C. Reverdin,[1] W. Seka,[2] and V. Tassin[1]
[1]*CEA, DAM, DIF, F-91297 Arpajon, France*
[2]*Laboratory for Laser Energetics, University of Rochester, Rochester, New York 14623-1299, USA*
[3]*Plasma Science and Fusion Center, Massachusetts Institute of Technology, Cambridge, Massachusetts 02139, USA*
[4]*Physics Department, University of Nevada, Reno, Nevada 89557, USA*
[5]*CEA, CVA, 21120 Is-sur-Tille, France*

(Received 29 September 2015; accepted 31 December 2015; published online 14 January 2016)

We present in this article direct-drive experiments that were carried out on the Omega facility [T. R. Boehly *et al*., Opt. Commun. **133**, 495 (1997)]. Two different pulse shapes were tested in order to vary the implosion stability of the same target whose parameters, dimensions and composition, remained the same. The direct-drive configuration on the Omega facility allows the accurate time-resolved measurement of the scattered light. We show that, provided the laser coupling is well controlled, the implosion time history, assessed by the "bang-time" and the shell trajectory measurements, can be predicted. This conclusion is independent on the pulse shape. In contrast, we show that the pulse shape affects the implosion stability, assessed by comparing the target performances between prediction and measurement. For the 1-ns square pulse, the measured neutron number is about 80% of the prediction. For the 2-step 2-ns pulse, we test here that this ratio falls to about 20%. © *2016 AIP Publishing LLC*. [http://dx.doi.org/10.1063/1.4939833]

I. INTRODUCTION

In Inertial Confinement Fusion (ICF) with laser, the implosion of the fuel-bearing capsule can be driven either directly by the laser ("direct-drive") or indirectly by a radiative flux, after the conversion of the laser energy to x-rays within a high-Z can called a hohlraum ("indirect-drive").[1] Independent of the drive, the coupling of the energy to the capsule can be an issue leaving the target implosion study with more questions than certainties. The implosion study, which is the purpose of the experiments presented in this article, relies on the knowledge of the energy that the capsule actually absorbs. One of the advantages of carrying out a laser direct-drive experiment is to allow the accurate time-resolved measurement of the laser energy coupling.[2] As we shall see in Section III, significant progress was made in these recent years in the understanding and in the control of the laser energy coupling.

For this reason, the direct-drive configuration is a perfect platform for the study of the implosion. The experiments presented here aim first to test our capacity to predict the implosion time history, which is determined by the implosion velocity. The time history main observable is the "bang-time," defined at the peak neutron production. Although the bang-time is a global observable that integrates the whole implosion, it remains a key observable. Very often, calculations are too optimistic, the calculated implosion velocity is too high, and the calculated bang-time occurs too early. Questions then occur about the drive or the energy the capsule actually absorbs. Here, the drive time-evolution is measured and known, which allows to focus on the implosion physics only. Thus, unpredicted bang-time different from predicted would indicate an inaccurate calculation of the implosion velocity. In the experiments presented in this article, the time-resolved ablation radius is also measured, which provides another information on the implosion. The implosion time history is discussed in Section IV.

Another important consideration is the implosion stability. It can be defined by the robustness of the configuration against all types of nonuniformities. Those are generated by the laser and target imperfections. Since the nonuniformities are not accounted for in the calculations, the comparison between predictions and measurements of the target performances provides a qualitative assessment of the stability of each configuration. It is from the perspective of a stability variation that we planned to study the implosion. From a configuration, we expect the pulse shape to be quite stable, whose impact on stability has already been demonstrated,[3–7] and is varied in order to move toward more unstable configurations. The capsule parameters (dimensions and compositions) remained the same in order to focus on only one parameter, i.e., the pulse shape. The expected stable configuration was designed based on the previous direct-drive studies that demonstrated an interest in thick ablators,[8] moderate gas fill,[9] and rapidly rising pulse:[3] 25 μm ablator thickness, 15 atm gas fill, and 1-ns square pulse. Other experiments are already planned in the future with thinner ablators and lower gas fills to continue the variations toward unstable configurations. The implosion stability is discussed in Section V.

The experimental setup is described in Section II before the laser coupling (Section III), the implosion time history (Section IV), and the implosion stability (Section V).

II. THE EXPERIMENTAL SETUP

The experiments described here were performed on the Omega facility.[10] The targets are gas-filled spherical plastic (CH) shells (Fig. 1). The thickness is 25 μm and the outer diameter is 930 μm. This high thickness was chosen to improve the stability.[8] Except for diagnostics requirements, the targets are the same for all the shots, which allows studying the implosion stability by varying the pulse shape only. Depending on the chosen diagnostics, they are filled with 15 atm of either pure deuterium (DD), or an equimolar mixture of deuterium and tritium (DT), or a mixture of 15 atm of deuterium and 0.07 atm of argon. All capsules are overcoated with a 0.1–μm aluminum gas retention barrier.

The capsules are irradiated by the 60 beams of Omega. The beams are smoothed by combining distributed phase plate (DPP), polarization smoothing (PS),[11] and smoothing by spectral dispersion (SSD).[12] The DPPs, called "SG04," have a super-Gaussian order of about ~4.12 with a radius at $1/e$ of peak intensity of about ~358 μm. Two pulse shapes are used (Fig. 1): a 1 ns square pulse (~26 kJ) or a two-step pulse (~23 kJ).

The large number of diagnostics is devoted to measuring the laser absorption, the shell trajectory, and the implosion performance. The scattered-light measurement is provided by two full-aperture backscattering stations (FABS) located in beams 25 and 30 and by two other channels located between focusing lenses.[2] These measurements are time-resolved and spectrally resolved. Each FABS station is also equipped with an absolutely calibrated calorimeter. These two calorimeters provide cross-calibration for four other calorimeters and for all time-resolved scattered-light spectra. The laser absorption is inferred from the scattered-light measurement, with an uncertainty of 5%. Also, the $\omega_0/2$ spectrum, where ω_0 is the laser frequency, is recorded. The spectral redshifted feature provides an electron-temperature diagnostic close to the $n_c/4$ surface, where n_c is the critical density.[13] The uncertainty is 0.15 keV.

The ablation front trajectory is obtained using the self-emission shadowgraphy technique.[14] Soft x-rays (~ 1 keV) are imaged with a pinhole array onto a four-strip x-ray framing camera (XRFC). This results in 16 time-resolved images (4 per strip). Each image is time integrated over 40 ps. The image-to-image timing is known within ± 2.5 ps and the absolute timing within $\pm 10\,ps$.[15,16] The ablation surface trajectory is inferred from the measurement of the steep inner edge in the self-emission images, and the averaged ablation front radius is known with an uncertainty of 0.15 μm.

The implosion performance is determined with the typical nuclear diagnostics. The neutron yield and the ion temperature are measured with the neutron time-of-flight (nTOF) diagnostics,[17] with uncertainties of, 6% and 0.5 keV. The time of peak neutron production, called "bang-time," is determined with an uncertainty of 100 ps by the neutron bang time diagnostics.[18] The shell areal density is inferred either from the number of knock-on protons, which are elastically scattered from the shell by 14.1 MeV DT neutrons, or from the secondary proton spectra in case of DD or DDAr gas fill. They are measured with magnet-based charged-particle spectrometers (CPS), with an uncertainty of about 15%.[19]

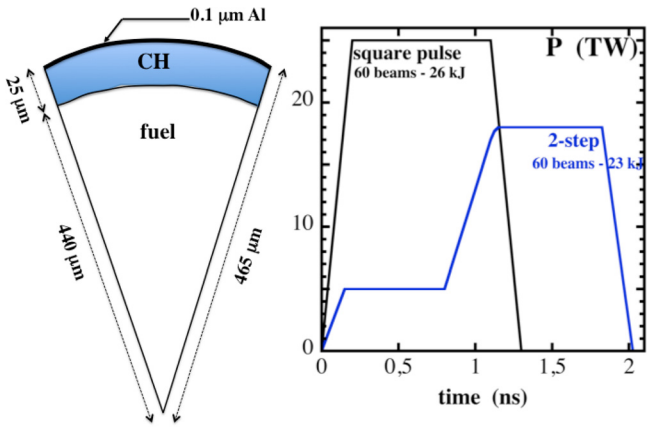

FIG. 1. Target and laser pulses. Depending on the choice of diagnostics, fuel is DT, or DD, or DD-Ar. The nominal gas fill is 15 atm. For DD-Ar, the nominal partial pressures are 15 atm of deuterium and 0.07 atm of argon. Two pulses are used.

III. LASER COUPLING

Knowing accurately the energy that a capsule actually absorbs is essential. So far, it has been an issue of concern in both the indirect-drive[20] and the direct-drive[21] configurations. The performances and the time history of the implosion depend on the energy absorbed by the capsule. For this reason, it is crucial that the unabsorbed laser energy be measured in these experiments.

One advantage of the direct-drive configuration is the capability to assess the absorbed drive energy or more precisely the scattered time-resolved energy. It is measured by the FABS and by two other channels (see Section II). The time-resolved laser absorption is inferred from this measurement.

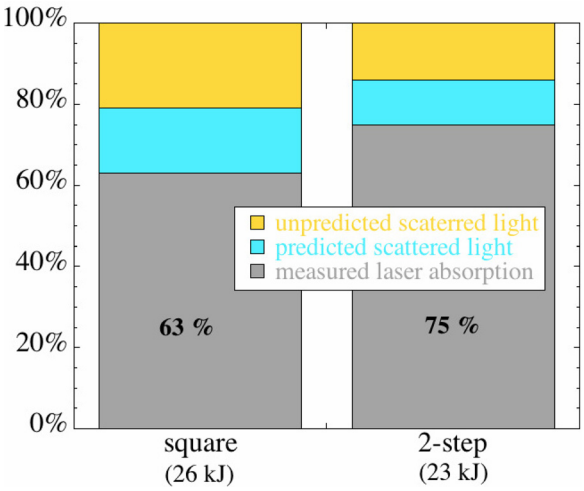

FIG. 2. Laser absorption fraction inferred from the measurements (grey) and scattered laser fraction from the 2D calculations (blue) for the two pulses. In yellow, the subtraction of the latter. In other words, this is the scattered laser that 2D calculations are unable to predict. Here, 2D calculations are performed with a nonlocal thermal conduction model,[23] without cross beam energy transfer.

Typically, a direct-drive capsule absorbs 60%–80% on the laser energy, depending on the pulse shape (Fig. 2). The higher the laser intensity, the lower the absorption. Thus, the square pulse absorption (∼63%) is lower than that of the shaped pulse (∼75%).

The laser absorption measurement has to be assessed by the calculation. Significant progress has been made recently in modeling absorption. According to Ref. 22, two models are required: a nonlocal thermal conduction model[23] and a Cross Beam Energy Transfer (CBET) model.[24]

In the hydrodynamic codes, the thermal conduction is usually modeled by the Spitzer-Härm theory, often combined with a flux-limiter.[25] But it has been known for several years that a flux-limited thermal conduction model is not consistent with all experimental observables.[21] A nonlocal model is an improvement of this theory and allows accounting for the nonlocal aspect of the electron thermal conduction,[26] without using flux-limiters. In our 2D hydrodynamic code, FCI2,[27] we use the model proposed by Schurtz-Nicolaï-Busquet (SNB).[23]

The CBET is a mechanism which transfers energy from the central portion of the laser beams to the edges of the beams propagating away from the target. It reduces the laser coupling to the target. Few hydrodynamic codes in the world are capable to account for this mechanism in a direct-drive configuration.[24,28] No CBET model is implemented in the FCI2 code.

With a nonlocal model and without CBET, the 2D calculated scattered energy (blue in Fig. 2) is about half of the measured scattered energy (blue + yellow in Fig. 2). The other half is not predicted by the 2D calculations. In other words, these calculations overpredict the laser absorption: 84% instead of 63% measured with the square pulse and 89% instead of 75% measured with the 2-step pulse.

Here, at least two strategies can be envisioned. First, we can choose to strongly limit the thermal conduction with flux-limiters $f \sim 0.05 - 0.06$ (with a sharp cutoff). A strong thermal conduction limitation steepens the density gradient which reduces the absorption and results in a bang-time quite close to the measurements. Direct-drive calculations were performed this way before the nonlocal models were implemented in hydrodynamic codes.[3,29] But, as mentioned earlier, it has already been demonstrated that this model is not consistent with all experimental observables.[21] Figs. 3–5 lead to the same conclusion. They confirm that even if a strong conduction limitation allows the calculations to match the measured absorbed energy (not the power) and the measured bang-time, it is unable to explain all the experimental observables (see the orange lines in Figs. 3–5).

Therefore, instead of strongly limiting the thermal conduction, we preferred to retain the nonlocal model and to reduce the incident laser power in the calculations, as it has been already done in other direct-drive studies[30,31] or, more recently in Ref. 32. The study presented here differs from the two first references not only in that we do not use flux-limiters but also in that the laser power reduction is calculated to match the measured laser absorption, not the bang-time. Another difference is that the reduction factor is time-resolved (defined by 6 points, actually). This way, compared

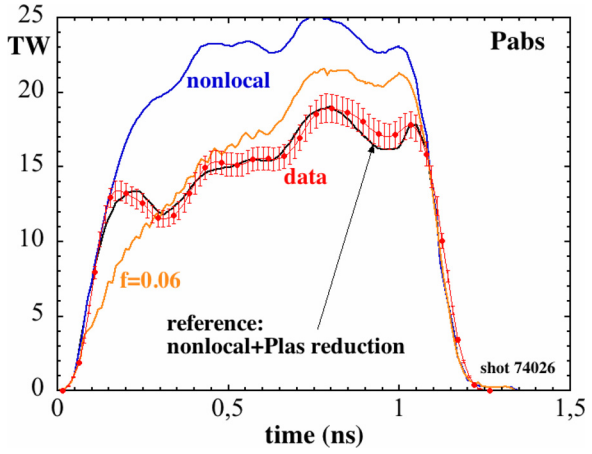

FIG. 3. Laser absorption versus time. The data (red points) are compared with 2D calculations: nonlocal model without laser reduction (blue), nonlocal model with laser reduction (black line), and flux-limiter of 0.06 without laser reduction (orange).

with the studies with nonlocal and CBET models, we replace the effects of the CBET by a time-resolved reduction of the laser power.

The study published in Ref. 32 follows an analogous approach: hydrodynamic calculations are performed with a nonlocal electron transport model and part of the incident laser power is withdrawn in order to account for CBET. But contrary to the configuration presented here, the implosion is not 1D and the equatorial power only is reduced to match the measured asymmetry.

An example of calculated time-resolved absorption is given in Fig. 3. Three calculations are compared with the data. First, a nonlocal calculation without incident laser reduction overpredicts the absorption, as was already shown in Fig. 2. Then, the absorption calculated with a flux-limiter and without incident laser reduction departs from the data: too low during the first half of the drive and too high during the second half. Note that this calculation exhibits time-integrated absorption and bang-time similar to the data. Our reference calculation, with a nonlocal model and a reduction of the incident laser power, exhibits as expected about the same absorption as the measurements: the laser reduction, 71% on an average, was designed with this objective.

The corona electronic temperature, Te, depends strongly on the laser coupling and on the thermal conduction model. The temperature at nc/4 can be inferred from the $\omega_0/2$ spectrum (see Section II), which permits comparing the validity of different thermal conduction models. The nonlocal calculation without incident laser reduction overpredicts the electronic temperature (Fig. 4). It was predictable as this calculation already overpredicts the laser absorption: too much laser absorption results in too much temperature in the corona. Another result which was less predictable is the big departure between the data and the flux-limiter calculation even though the absorbed energies are about the same. The Te calculated at nc/4 with flux limitation is well above the measurement: 2.8 keV instead of 2.4 keV. It arises from the strong thermal conduction limitation which retains the energy in the corona and thus maintains the corona

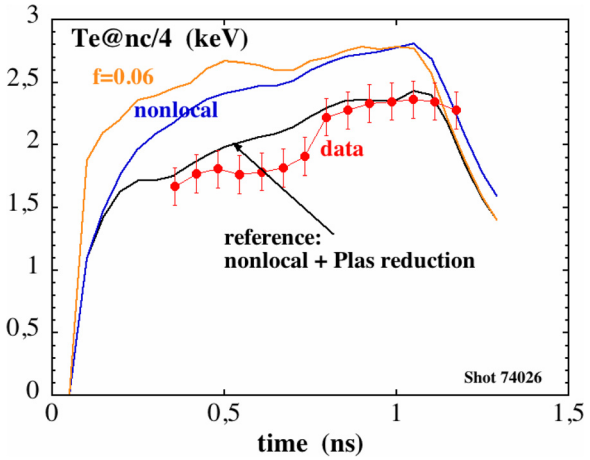

FIG. 4. Te inferred at nc/4 versus time. Same legend as in Fig. 3.

temperature at a high level. This result definitively eliminates the strong conduction limitation option. Finally, the Te calculated with the nonlocal model and a laser reduction is very close to the measurement.

These good agreements validate our strategy: nonlocal model and reduction of the incident laser to match the measured time-resolved laser absorption. It is confirmed by the comparison of the ablation radii (see below).

IV. IMPLOSION TIME HISTORY

The first observable of the implosion velocity is the time of peak neutron-production, the "bang-time," which gives only a global information on the implosion history. It would be ideal to follow the shock propagation inside the target, but we do not have that type of diagnostic here. A time history information is provided by the ablation surface trajectory measurement inferred from the corona self-emission (see Section II), but available only during the laser duration.

The ablation radii inferred from the measurement and from different 2D calculations are compared in Fig. 5. The conclusions are the same as from the comparisons of laser absorption and electronic temperature. The nonlocal calculation without laser reduction, which overpredicts the laser absorption and thus the Te, results in too fast ablation. The

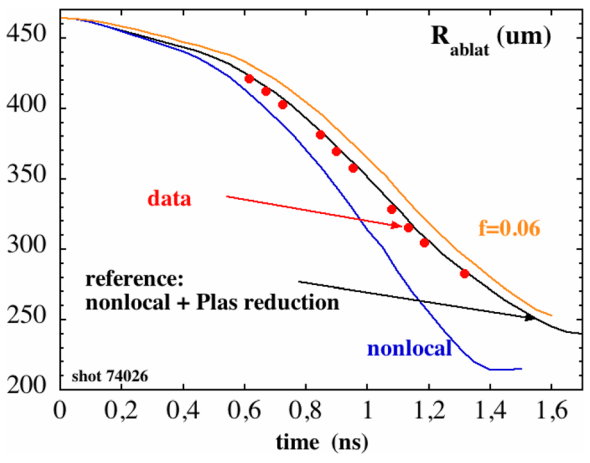

FIG. 5. Ablation radius versus time. Same legend as in Fig. 3.

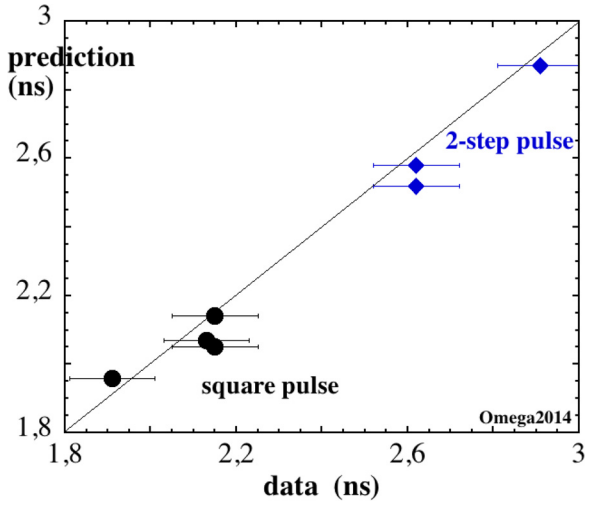

FIG. 6. 2D calculated bang-time as a function of the measured bang-time. The 2D calculations were performed with a nonlocal model and a reduction of the incident laser power to match the measured laser absorption.

strongly limited conduction calculation, which underpredicts the laser absorption at the beginning, leads to too low ablation. Again, we find a good agreement between the data and the calculation with the nonlocal model and the laser reduction, which is our reference calculation.

The agreement for the ablation surface trajectory is confirmed by the bang-time comparisons (Fig. 6). For all the shots, where the bang-time measurement was available, the reference calculation result lies inside the error bar of the data. Namely, we find here that, provided the laser coupling is controlled, the implosion velocity can be predicted. We confirm that the implosion history depends mainly on the power that the capsule actually absorbs.

Moreover, this conclusion is independent on the pulse shape: for the 2-step pulse which, as it is shown in Section V, leads to a more unstable implosion, the agreement for the bang-time is good. In other words, the implosion time history and the implosion stability are independent for the configurations studied here: warm capsule with a high ablator thickness.

V. STABILITY AND PERFORMANCES

The implosion stability is the robustness of the implosion against all possible perturbations seeded by the laser irradiation (power imbalance, beam nonuniformities, and beam mispointing) or by the target imperfections (roughness and deformations).[33] These perturbations grow during the implosion and can compromise the target performances.

None of these nonuniformities are accounted for in our 2D calculations. Consequently, the comparison between prediction and measurement provides a qualitative measure of configuration stability: a good agreement will be the signature of a stable configuration. Inversely, an unstable implosion will depart significantly from the predictions. The target performances measured in these experiments are the fuel ion temperature, Ti, the areal density, ρR, and mainly the neutron production.

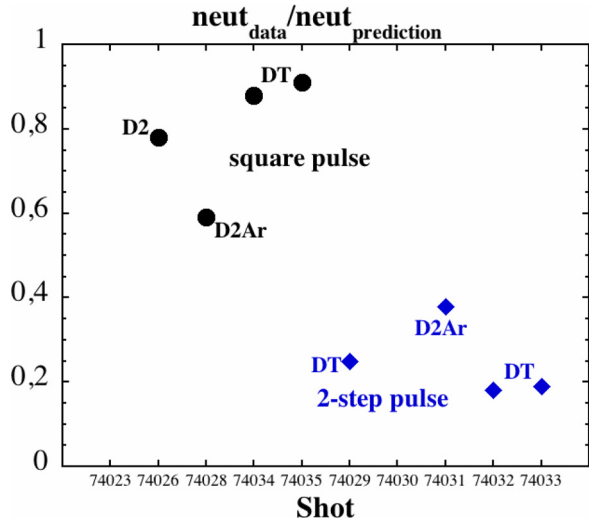

FIG. 7. Yield Over 2D Simulation (YOS) as a function of the shot number. The YOS is the measured number of neutrons divided by the 2D calculated number of neutrons. The measured DT neutrons are 3×10^{12} for the square pulse and 2×10^{12} for the 2-step pulses. The number is about 50 times lower in case of DD gas fill and 100 times lower in case of DDAr.

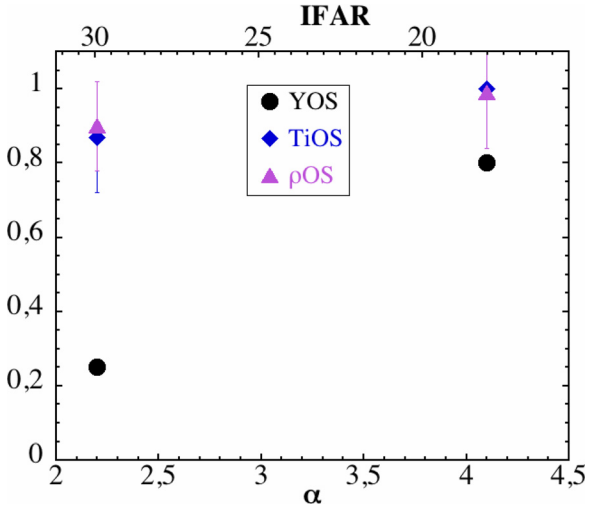

FIG. 8. Ratio of the measurement to the calculations for the yield (solid circles), the fuel temperature (solid diamonds), and the areal density (solid triangles) versus the adiabat and the IFAR.

The interesting result is that we observe no correlation between the implosion stability and the implosion time history. As shown in Section IV, a good agreement between calculations and measurements was found for the bang-time, suggesting that the implosion velocity is well predicted. However, we will see in this section that the accurate prediction of the implosion velocity does not result in a good agreement for the implosion performances.

The first measurement of the implosion stability appears to be the Yield Over Simulation (YOS), that is the ratio of measured neutrons to the 2D calculated neutrons (Fig. 7). A YOS close to 1 indicates a relative stable implosion.

The trend of lower YOS and lower stability for the 2-step pulse is evident. YOS is about 80% for the square pulse and falls down to about 20% for the 2-step pulse. Note that for all the shots, the calculated shock yield proportion is very low, $\sim 1\% - 2\%$ for the square pulse and $\sim 0.5\%$ for the 2-step pulse. The yield comes primarily from the fuel compression by the shell.

As expected, based on the previous direct-drive studies, the square pulse configuration is the stable configuration. It is also consistent with the values of the three key stability parameters calculated for both pulses (Table I). First, the adiabat, defined as the ratio of the pressure to the Fermi-degenerate pressure, is a metric of the entropy delivered to the shocked material. It is mainly determined by the pulse shape and the laser intensity: a rapidly rising pulse places the shell on a higher adiabat. α ranges from 2.2 for the 2-step pulse to 4.1 for the square pulse. Since the adiabat has a stabilizing effect on the Rayleigh-Taylor instability at the ablation front,[34–37] the higher the adiabat, the more stable is the implosion.

TABLE I. Key stability parameters for the two pulses. α is the minimum value of the adiabat in the shell at stagnation. C_r is the ratio of the initial fuel radius to the minimum fuel radius (stagnation). IFAR is the maximum value of the "in flight aspect ratio," after the first shock breaks out into the fuel. It is about the time when the second shock breaks out. At this time, the shell radius is $\sim 3/4 - 4/5$ of the initial radius.

	Square	2-step
α	4.1	2.2
C_r	14	16
IFAR	18	30

Another stability metric which explains the trend observed in Figure 7 is the "in-flight aspect ratio" defined as $IFAR = R/\Delta R$, where R is the shell radius and ΔR is the in-flight shell thickness. The growth rates for the most dangerous mode scale as $\sqrt{IFAR}$.[38] The lower the in flight aspect ratio (IFAR), the more stable is the implosion. The maximum value of IFAR during the acceleration phase ranges from $\approx$18 (square pulse, stable configuration) to $\approx$30 (2-step pulse, less stable configuration).

The last stability parameters assessed here is the convergence ratio, C_r, defined as the ratio of the initial fuel radius to the minimum fuel radius. The perturbations growth at the interface during the shell deceleration phase increases with C_r.[39] And like IFAR, the convergence ratio depends on the laser energy and also on the target configuration, precisely on the gas fill.[4] Since the gas fill is the same for all the shots, the C_r variations are too small here to be significant: C_r is 14 for the square pulse and 16 for the 2-step pulse.

Unsurprisingly, the calculated values of the main stability parameters point out the square pulse as the stable configuration (high adiabat, low IFAR) and the 2-step pulse configuration as a less stable configuration (lower adiabat, higher IFAR).

The comparison of the fuel temperatures Ti, measured and calculated from the Doppler width of the 14 Mev neutrons,[40] confirms the YOS assessment (Fig. 8): the more stable configuration (square pulse, $\alpha \approx 4$, $IFAR \approx 18$) brings the prediction closer to the data than for the less stable configurations (2-step pulse, $\alpha \approx 2.2$, $IFAR \approx 30$). Fig. 8 shows that the discrepancy between predictions and measurements, and the variations versus the stability, are lower for T_i than

for the yield. It arises from the high sensibility of the neutron production on the ion temperature. For these fuel temperature (about 2 keV), the number of neutrons varies as $\sim\rho^2 T_i^4$.

The comparison of the areal densities leads also to the same conclusion (see Fig. 8). The calculation is closer to the measurement for the more stable configuration ($\alpha \approx 4$, $IFAR \approx 18$). Thus, the target performances we examine here, the yield, the fuel temperature, and the areal density, clearly depend on the acceleration phase stability metrics, the adiabat, and IFAR. Other experiments are already planned with thinner ablator, in order to further investigate higher IFAR configurations, and lower gas fills, which will provide significant variations in the convergence.

VI. CONCLUSIONS

A direct-drive campaign with 2 different pulses shapes and one target configuration was performed. We show that provided the laser coupling is well controlled, the implosion time history, and therefore the implosion velocity, can be predicted. Without CBET model, the control of the laser coupling relies on the time-resolved scattered laser measurement. Moreover, the reliability of the laser coupling prediction is independent of the two pulse shapes used. In contrast, the stability of the implosion clearly depends on the pulse shape, although the implosion velocity is well predicted. A short pulse, with a fast rise, results in more shell entropy and achieves less convergence. In these conditions, the calculated performances, neutron production, Ti, and areal density, are close to the data. The measured number of neutrons is 80% of the prediction (YOS = 80%). This 1-ns square pulse can be considered stable. Inversely, a 2-step pulse lowers the entropy and achieves bigger convergence. This configuration is more unstable and the calculated performances are too much optimistic. YOS is ~20%. Other direct-drive campaigns are already planned with the variations of the target parameters.

ACKNOWLEDGMENTS

The authors acknowledge the LLE facility where the experiments described here were carried out.

[1]S. Atzeni and J. Meyer-ter-Vehn, *The Physics of Inertial Fusion* (Oxford University Press, Oxford, 2004).
[2]W. Seka, D. H. Edgell, J. P. Knauer, J. F. Myatt, A. V. Maximov, R. W. Short, T. C. Sangster, C. Stoekl, R. E. Barr, R. S. Craxton *et al.*, Phys. Plasmas **15**, 056312 (2008).
[3]F. Marshall *et al.*, "Direct-drive hollow-shell implosion studies on the 60-beam UV OMEGA laser system," Phys. Plasmas **7**, 1006 (2000).
[4]F. J. Marshall, J. A. Delettrez, R. Epstein, V. Yu. Glebov, D. R. Harding, P. W. McKenty, D. D. Meyerhofer, P. B. Radha, W. Seka, S. Skupsky, V. A. Smalyuk *et al.*, Phys. Plasmas **7**, 2108 (2000).
[5]V. N. Goncharov, J. P. Knauer, P. W. McKenty, P. B. Radha, T. C. Sangster, S. Skupsky, R. Betti, R. L. McCrory, and D. D. Meyerhofer, Phys. Plasmas **10**, 1906 (2003).
[6]X. Ribeyre, Ph. Nicolai, G. Schurtz, M. Olazabal-Loume, J. Breil, P. H. Maire, J. L. Feugeas, L. Hallo, and V. T. Tikhonchuk, Plasma Phys. Controlled Fusion **50**, 025007 (2008).
[7]P. B. Radha, C. Stoeckl, V. N. Goncharov, J. A. Delettrez, D. H. Edgell, J. A. Frenje, I. V. Igumenshchev, J. P. Knauer, J. A. Marozas, R. L. McCrory *et al.*, Phys. Plasmas **18**, 012705 (2011).
[8]S. P. Regan, J. A. Delettrez, V. N. Goncharov, F. J. Marshall, J. M. Soures, V. A. Smalyuk, P. B. Radha, B. Yaakobi, R. Epstein, V. Yu. Glebov *et al.*, Phys. Rev. Lett. **92**, 185002 (2004).
[9]D. D. Meyerhofer, J. A. Delettrez, R. Epstein, V. Yu. Glebov, V. N. Goncharov, R. L. Keck, R. L. McCrory, P. W. McKenty, F. J. Marshall, P. B. Radha *et al.*, Phys. Plasmas **8**, 2251 (2001).
[10]T. R. Boehly, D. L. Brown, R. S. Craxton, R. L. Keck, J. P. Knauer, J. H. Kelly, T. J. Kessler, S. A. Kumpan, S. J. Loucks, S. A. Letzring *et al.*, Opt. Commun. **133**, 495 (1997).
[11]J. E. Rothenberg, J. Appl. Phys. **87**, 3654 (2000).
[12]S. Skupsky, R. W. Short, T. Kessler, R. S. Craxton, S. Letzring, and J. M. Soures, J. Appl. Phys. **66**, 3456 (1989).
[13]W. Seka, J. F. Myatt, R. W. Short, D. H. Froula, J. Katz, V. N. Goncharov, and I. V. Igumenshchev, Phys. Rev. Lett. **112**, 145001 (2014).
[14]D. T. Michel, C. Sorce, R. Epstein, N. Whiting, I. V. Igumenshchev, R. Jungquist, and D. H. Froula, Rev. Sci. Instrum. **83**, 10E530 (2012).
[15]D. T. Michel, V. N. Goncharov, I. V. Igumenshchev, R. Epstein, and D. H. Froula, Phys. Rev. Lett. **111**, 245005 (2013).
[16]D. T. Michel, A. K. Davis, W. Armstrong, R. Bahr, R. Epstein, V. N. Goncharov, M. Hohenberger, I. V. Igumenshchev, R. Jungquist, D. D. Meyerhofer *et al.*, High Power Laser Sci. Eng. **3**, E19 (2015).
[17]V. Yu. Glebov, C. Stoeckl, T. C. Sangster, S. Roberts, G. J. Schmid, R. A. Lerche, and M. J. Moran, Rev. Sci. Instrum. **75**, 3559 (2004).
[18]C. Stoeckl, V. Yu. Glebov, J. D. Zuegel, D. D. Meyerhofer, and R. A. Lerche, Rev. Sci. Instrum. **73**, 3796 (2002).
[19]C. K. Li, F. H. Seguin, D. G. Hicks, J. A. Frenje, K. M. Green, S. Kurebayashi, R. D. Petrasso, D. D. Meyerhofer, J. M. Soures, V. Yu. Glebov *et al.*, Phys. Plasmas **8**, 4902 (2001).
[20]S. A. MacLaren, M. B. Schneider, K. Widman, J. H. Hammer, B. E. Yoxall, J. D. Moody, P. M. Bell, L. R. Benedetti, D. K. Bradley, M. J. Edwards *et al.*, Phys. Rev. Lett. **112**, 105003 (2014).
[21]S. P. Regan, R. Epstein, V. N. Goncharov, I. V. Igumenshchev, D. Li, P. B. Radha, H. Sawada, W. Seka, T. R. Boehly, J. A. Delettrez *et al.*, Phys. Plasmas **14**, 056305 (2007).
[22]D. H. Froula, I. V. Igumenshchev, D. T. Michel, D. H. Edgell, R. Follett, V. Yu. Glebov, V. N. Goncharov, J. Kwiatkowski, F. J. Marshall, P. B. Radha *et al.*, Phys. Rev. Lett. **108**, 125003 (2012).
[23]G. Schurtz, Ph. D. Nicolaï, and M. Busquet, Phys. Plasmas **7**, 4238 (2000).
[24]I. V. Igumenshchev, W. Seka, D. H. Edgell, D. T. Michel, D. H. Froula, V. N. Goncharov, R. S. Craxton, L. Divol, R. Epstein, R. Follet *et al.*, Phys. Plasmas **19**, 056314 (2012).
[25]R. C. Malone, R. L. McCrory, and R. L. Morse, Phys. Rev. Lett. **34**, 721 (1975).
[26]J. F. Luciani, P. Mora, and J. Virmont, Phys. Rev. Lett. **51**, 1664 (1983).
[27]D. Besnard, G. Bonnaud, and G. Schurtz, *La Fusion Thermonucleaire Par Laser*, edited by R. Dautray and J. P. Watteau (Eyrolles, Paris 1993), Pt. 3, Vol. 2, p. 1117.
[28]A. Colaitis, G. Duchateau, P. Nicolaï, and V. Tikhonvhuk, Phys. Rev. E **89**, 033101 (2014).
[29]B. Canaud, F. Garaude, P. Ballereau, J. L. Bourgade, C. Clique, D. Dureau, M. Houry, S. Jaouen, H. Jourdren, N. Lecler *et al.*, Plasma Phys. Controlled Fusion **49**, B601 (2007).
[30]E. S. Dodd, J. F. Benage, G. A. Kyrala, D. C. Wilson, F. J. Wysocki, W. Seka, V. Yu. Glebov, C. Stoeckl, and J. A. Frenje, Phys. Plasmas **19**, 042703 (2012).
[31]A. R. Miles, H.-K. Chung, R. Heeter, W. Hsing, J. A. Koch, H.-S. Park, H. F. Robey, H. A. Scott, R. Tommasini, J. Frenje *et al.*, Phys. Plasmas **19**, 072702 (2012).
[32]T. J. Murphy, N. S. Krasheninnikova, G. A. Kyrala, P. A. Bradley, J. A. Baumgaertel, J. A. Cobble, P. Hakel, S. C. Hu, J. L. Kline, D. S. Montgomery *et al.*, Phys. Plasmas **22**, 092707 (2015).
[33]P. B. Radha, T. J. B. Collins, J. A. Delettrez, Y. Elbaz, R. Epstein, V. Yu. Glebov, V. N. Goncharov, R. L. Keck, J. P. Knauer, J. A. Marozas *et al.*, Phys. Plasmas **12**, 056307 (2005).
[34]S. E. Bodner, Phys. Rev. Lett. **33**, 761 (1974).
[35]R. Betti, V. N. Goncharov, R. L. McCrory, and C. P. Verdon, Phys. Plasmas **5**, 1446 (1998).
[36]V. N. Goncharov, P. W. McKenty, S. Skupsky, R. Betti, R. L. McCrory, and C. Cherfils-Clerouin, Phys. Plasmas **7**, 5118 (2000).
[37]K. Anderson and R. Betti, Phys. Plasmas **10**, 4448 (2003).
[38]C. D. Zhou and R. Betti, Phys. Plasmas **14**, 072703 (2007).
[39]V. A. Smalyuk, J. A. Delettrez, V. N. Goncharov, F. J. Marshall, D. D. Meyerhofer, S. P. Regan, T. C. Sangster, R. P. J. Town, and B. Yaakobi, Phys. Plasmas **9**, 2738 (2002).
[40]D. Riz, F. Garaude, M. Houry, and B. Canaud, Nucl. Fusion **46**, 864 (2006).